AIR POLLUTION

Fires reverse progress toward ozone air quality standards in the United States

Weizhi Deng[1], Jun Wang[1]*, Meng Zhou[2]*, Xi Chen[1], Xiaodong Wu[3], Huanxin Zhang[1], Jason B. Cohen[4], Jing Wei[5], Arlindo da Silva[2], Guy P. Brasseur[6,7], Claire Granier[8,9], Laurence Rouil[10]

Recent surges in wildfire emissions have exacerbated surface ozone pollution in the United States. Using deep learning, we developed a gapless daily surface ozone dataset at 1-kilometer resolution for 2003–2024. This dataset revealed a reversal in national policy–relevant ozone trends that had gone undetected by the sparse monitoring network: from −0.65 parts per billion (ppb) per year (2003–2015) to +0.13 ppb per year (2015–2024). The reversal was primarily driven by increasing wildfire emissions, offsetting 3.9 years of mitigation progress. Premature deaths from fire-sourced ozone have increased by 318 deaths per year since 2013, with post-2013 mortality 46% higher than pre-2013 mortality. During 2022–2024, wildfire emissions exposed 43 million people to nonattainment conditions, effectively preventing a 4-ppb tightening of the ozone standard. These results underscore the growing challenges of sustaining air quality progress as wildfires intensify under climate change.

Despite regulated reductions in anthropogenic emissions of ozone (O_3) precursors, observation stations indicate that policy-relevant surface O_3 levels have plateaued since 2013 (*1*), a finding that is potentially linked to increasing fire emissions from the western US and Canada (*2*–*6*). This stagnation poses challenges to meet and potentially tighten the 2015 US National Ambient Air Quality Standards (NAAQS), which set a health-based limit of 70 parts per billion (ppb) for O_3, expressed as the annual fourth-highest maximum daily 8-hour average (MDA8) O_3 averaged over 3 years (*7*). However, efforts to inform regulatory policy are largely hindered by sparse ground measurements: US Environmental Protection Agency (EPA) monitoring stations cover just 2% of the land area in the continental US (CONUS), assuming a 10-km radius per station, and serve only 26% of the population (Fig. 1A). As a result, NAAQS attainment status is often designated at the county level and cannot even be determined for many regions (*8*). The incomplete spatial coverage of the ground monitoring network also challenges the estimates of O_3 exposure and associated mortality, which require gapless MDA8 data at high resolution to convolve with fine-scale population data (*9*, *10*). Furthermore, only 35% of the stations (723 of 2037) have continuous records from 2003 to 2024 (Fig. 1A), limiting the representativeness of the long-term trend derived from this sparse network (*11*, *12*).

Here, we used deep learning to generate a full-coverage, high-resolution (1 km), long-term (2003–2024) daily MDA8 dataset across CONUS, with a focus on exceedance events relevant to NAAQS. We then conducted full-coverage neighborhood-scale NAAQS assessments, quantified fire impacts on the long-term trends of policy-relevant O_3 levels and associated all-cause premature mortality, and evaluated the feasibility of implementing stricter standards, providing critical insights for O_3 policy amid increasing fire emissions.

Full-coverage O_3 mapping by means of deep learning

Although machine learning (ML) has gained traction in generating gapless atmospheric datasets, long-term ML-based MDA8 datasets are not available over CONUS after 2016 (*13*, *14*), and thus, data for recent years of heightened wildfire emissions are missing (*5*, *15*). Furthermore, existing ML studies tend to underestimate MDA8 values during extreme events (MDA8 >70 ppb), often by 50 to 80%, partly because of training biases that favor lower values (table S1). This underestimation is reflected in regression slopes that are less than unity when comparing ML predictions with observations, leading to a substantial undercounting of exceedance days.

To address these limitations, we developed a multilayer perceptron (MLP) model with a custom cost function that assigns higher weights to extreme events that are rare in the training distribution (methods). The MLP model was trained on EPA daily MDA8 measurements as the target variable, with features from atmospheric composition reanalysis, meteorological reanalysis, and satellite remote-sensing products (table S2). In particular, we used surface O_3 and precursor concentrations from the Copernicus Atmosphere Monitoring Service (CAMS) reanalysis, which is based on a chemical transport model driven by emission inventories constrained by extensive assimilation of satellite aerosol and trace gas observations (*16*). To further downscale the model from CAMS's native resolution (75 km) to 1 km for fine-scale attainment and exposure assessments, we incorporated high-resolution remotely sensed features that represent local variability in emissions and surface characteristics. These include LandScan population density (*17*), Visible Infrared Imaging Radiometer Suite (VIIRS) nighttime light intensity (*18*), Moderate Resolution Imaging Spectroradiometer (MODIS) normalized difference vegetation index (NDVI) (*19*), Advanced Spaceborne Thermal Emission and Reflection Radiometer (ASTER) topography elevation (*20*), and MODIS land cover type (*21*).

We validated our model based on out-of-sample fivefold cross-validation (methods) and compared its performance against benchmark CAMS reanalysis (Fig. 1, D and E). CAMS explains 53% of the total variability in EPA daily MDA8 measurements, with a root mean square error (RMSE) of 11.07 ppb and a mean bias (MB) of +4.38 ppb. It tends to overestimate lower values (<50 ppb) and underestimate extremes (>70 ppb), with a regression slope of 0.76. By contrast, the MLP demonstrates considerable improvements, with a coefficient of determination (R^2) of 0.88 (66.0% increase), an RMSE of 4.89 ppb (55.8% reduction), and an MB of −0.03 ppb (99.3% reduction). These improvements are important for accurately estimating the O_3-related health burden because the positive bias in CAMS would inflate mortality estimates, whereas the MLP largely eliminates the overall bias. The MLP also improves prediction of exceedance events, increasing the hit rate from 45.8 to 75.3% (+2.5 exceedance events per station per year) and reducing the false alarm ratio from 74.5 to 39.7% (−7.5 false alarms per station per year). These advancements, including a regression slope of 0.98, are crucial for evaluating NAAQS compliance, where exceedance events should not occur more than three times per year on average at a given station. Out-of-station fivefold cross-validated results also confirm the model's improvements in predicting extreme events, indicated by a regression slope of 0.90 (fig. S1). Further evaluations on a site-by-site and year-by-year basis are given in the supplementary text.

[1]Department of Chemical and Biochemical Engineering, The University of Iowa, Iowa City, IA, USA. [2]Global Modeling and Assimilation Office, NASA Goddard Space Flight Center, Greenbelt, MD, USA. [3]Department of Electrical and Computer Engineering, The University of Iowa, Iowa City, IA, USA. [4]Independent Researcher, New Brunswick, NJ, USA. [5]Department of Atmospheric and Oceanic Science, Earth System Science Interdisciplinary Center, University of Maryland, College Park, MD, USA. [6]Atmospheric Chemistry Observations and Modeling Laboratory, National Center for Atmospheric Research, Boulder, CO, USA. [7]Environmental Modeling Group, Max Planck Institute for Meteorology, Hamburg, Germany. [8]Laboratoire d'Aérologie, CNRS, Université de Toulouse, Toulouse, France. [9]Chemical Sciences Laboratory, NOAA/CIRES, University of Colorado, Boulder, CO, USA. [10]Copernicus Atmospheric Monitoring Service, European Centre for Medium-Range Weather Forecasts, Bonn, Germany. ***Corresponding author. Email: jun-wang-1@uiowa.edu (J.Wa.); mzhou16@umbc.edu (M.Z.)**

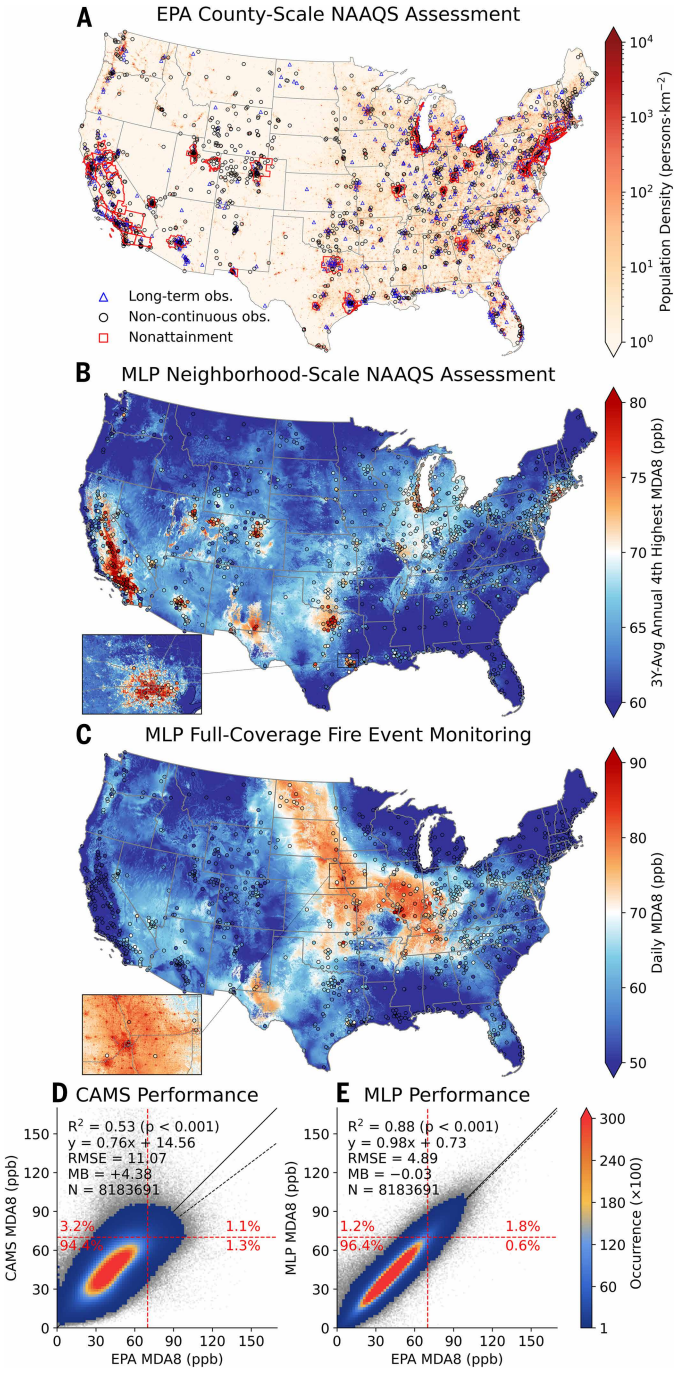

Fig. 1. Need for a long-term, full-coverage, high-resolution MDA8 O_3 dataset. (**A**) EPA stations overlaid on LandScan population density (blue triangles indicate stations with long-term observations from 2003 to 2024; black circles indicate stations missing at least 1 year of observations). Red polygons show the county-scale nonattainment regions designated by the EPA. (**B**) MLP-predicted annual fourth-highest MDA8 values averaged over 2022–2024 overlaid with EPA measurements, highlighting nonattainment regions (>70 ppb) at the neighborhood scale. (**C**) MLP-predicted daily MDA8 values overlaid with EPA measurements during a long-range wildfire-smoke transport event on 6 June 2023. (**D** and **E**) Performance of benchmark CAMS reanalysis and MLP prediction, respectively, validated against EPA daily MDA8 measurements. Black solid lines are 1:1 lines, black dashed lines are best fits, red dashed lines are the 2015 NAAQS standard, and color represents data density. MLP results are based on out-of-sample fivefold cross-validation.

We applied the MLP model across CONUS to produce gapless daily MDA8 estimates from 2003 to 2024, enabling a full-coverage NAAQS assessment (Fig. 1B). The MLP results capture nonattainment urban regions in California, Arizona, Utah, Colorado, Texas, Georgia, the Lake Michigan region, and the New York metropolitan area, consistent with EPA designations shown in Fig. 1A. In addition, the MLP-predicted dataset uncovers emerging regions of concern that could benefit from enhanced monitoring. For instance, it suggests that western Texas and southeastern New Mexico have been in nonattainment since 2018 because of increased oil and gas activities, as evidenced by enhanced gas flaring (*22*, *23*) and tropospheric NO_2 signals (*24*). Yet these regions remain undesignated by the EPA (Fig. 1A), highlighting the potential of the dataset to identify regions where expanded monitoring could be valuable.

Furthermore, the MLP captures O_3 variability at 1-km resolution, offering neighborhood-scale NAAQS assessments over traditional county-scale evaluations that were limited by EPA station density (*8*). A zoomed-in view over Houston shows that nonattainment areas align closely with densely populated zones (Fig. 1B). Such high-resolution assessment can be useful for guiding policy-makers toward more targeted and effective mitigation strategies. The high-resolution MLP results can also be combined with fine-scale population data to provide spatially resolved estimates of exposure and mortality burden compared with those directly using coarse-resolution chemical transport model outputs (*10*).

The MLP results also better capture wildfire-influenced perimeters, particularly in rural and remote areas underrepresented by EPA stations. Figure 1C shows the MLP-predicted MDA8 values during a long-range transport event of Canadian wildfire smoke on 6 June 2023. Smoke-induced O_3 enhancements are evident in North Dakota, South Dakota, Nebraska, and Iowa, extending southward into Oklahoma and eastward into Indiana and Tennessee, in good agreement with available station measurements. In areas with limited monitoring coverage, such as in Nebraska, where surface O_3 threatens not only human health but also agricultural productivity, the full-coverage MLP mapping is particularly valuable for resolving the extent of smoke-related O_3 impacts. These results highlight the importance of a long-term, full-coverage, high-resolution daily MDA8 dataset to inform O_3 policy.

O_3 trends and fire impacts

We evaluated trends of policy-relevant O_3 levels (i.e., 3-year running average of annual fourth-highest MDA8) across CONUS from 2003 to 2024 using our full-coverage MLP-predicted dataset and estimated fire impacts on O_3 trends. Although previous studies have reported wildfire-driven trend reversals for surface fine particulate matter based on EPA station measurements (*6*) or a full-coverage ML-based dataset (*4*), the role of wildfires in long-term surface O_3 trends has not been systematically assessed. We estimated wildfire impacts on O_3 trends using two approaches following previous studies (*4*, *25*) (methods). The first approach derives counterfactual "no-fire" trends by excluding days and locations affected by wildfires (*4*), identified through abnormally high surface carbon monoxide levels in CAMS reanalysis. The second approach applies paired GEOS-Chem chemical transport model simulations with and without fire emissions to estimate the relative fire contribution to O_3 (*25*, *26*). We then calculated fire-sourced O_3 as the product of MLP-predicted all-source O_3 and simulated fire relative contribution and obtained counterfactual "no-fire" O_3 levels by subtracting the fire-sourced O_3 from the total. The two methods yielded consistent counterfactual results [Pearson correlation coefficient (R) = 0.99; fig. S2], and we present the first approach in the paragraphs that follow.

Nationally, full-coverage MLP results reveal an O_3 trend reversal from a decline to an increase after 2015, primarily driven by increasing wildfire emissions (Fig. 2C). The trend breakpoint search algorithm

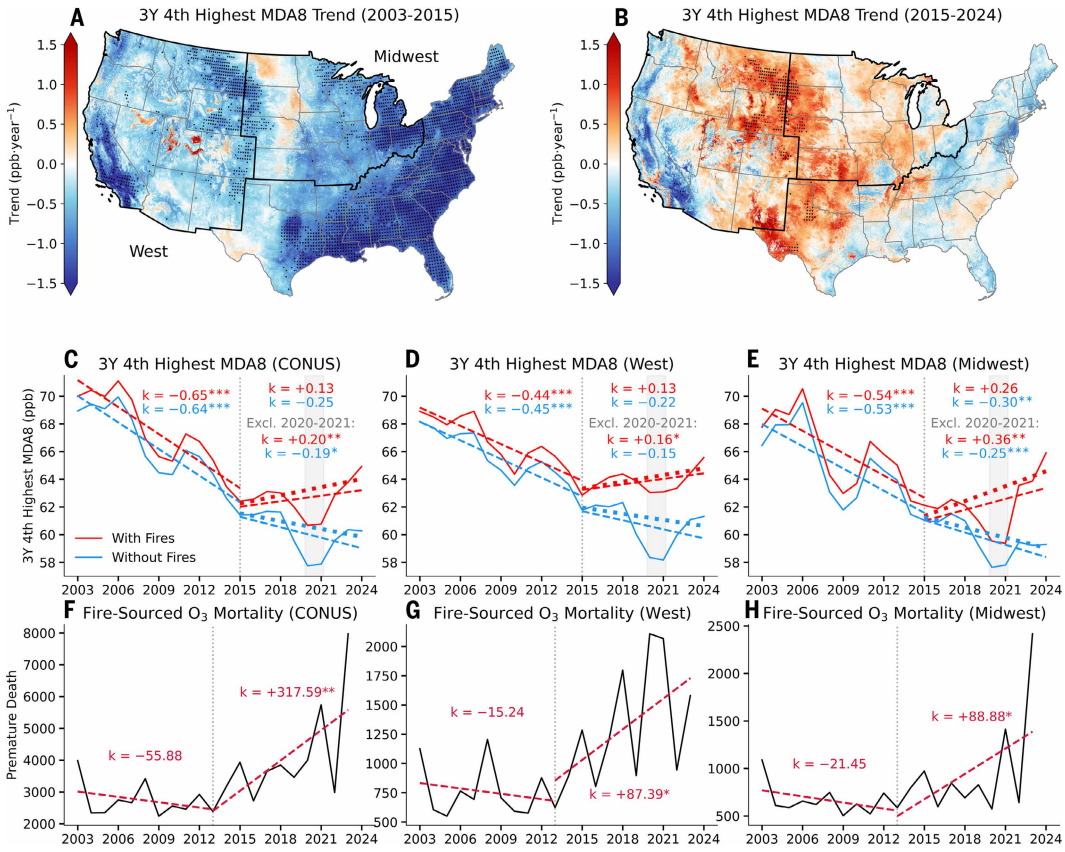

Fig. 2. Trends of policy-relevant O_3 levels and associated mortality amid declining anthropogenic emissions and increasing fire emissions. (**A** and **B**) Grid-level trends of policy-relevant O_3 levels during (A) 2003–2015 and (B) 2015–2024 based on MLP results. Policy-relevant O_3 levels are calculated as a 3-year running average of the annual fourth-highest MDA8 O_3 values (using 2 years at the edges). Black dots denote trends that are statistically significant at the 0.1 level. The western US and Midwest regions are outlined. (**C** to **E**) Time series (solid lines) and trends (dashed lines) of policy-relevant O_3 levels over (C) CONUS, (D) the western US, and (E) the Midwest. Red lines represent MLP-predicted values, and blue lines show counterfactual estimates excluding fire impacts. Gray shading marks the COVID-19 period (2020–2021). Bold dotted lines show post-2015 trends, excluding 2020–2021. Linear trend slopes *k* are annotated, with significance levels denoted by asterisks: $*P < 0.1$, $**P < 0.05$, and $***P < 0.01$. (**F** to **H**) Time series and trends of premature deaths attributable to fire-related long-term O_3 exposure over (F) CONUS, (G) the western US, and (H) the Midwest. Linear trend slopes and corresponding significance level are annotated as in (C) to (E).

(methods) detects two breakpoints for CONUS: 2015 and 2020. However, 2020 coincides with the COVID-19 pandemic, during which large reductions in anthropogenic emissions lowered policy-relevant O_3 levels by 3 to 4% (*27*), and thus may not represent a structural transition in long-term O_3 behavior. We therefore adopted 2015 as the primary breakpoint, as it reflects the onset of the longer-term trend shift associated with increasing wildfire influence under regulated anthropogenic emission reductions (supplementary text). From 2003 to 2015, policy-relevant O_3 levels decreased at a statistically significant rate of 0.65 ppb year^{-1} because of regulated reduction in anthropogenic precursor emissions (*28*). However, the trend reversed to positive during 2015–2024 (+0.13 ppb year^{-1}; or +0.20 ppb year^{-1} when the anomalous COVID-19 period is excluded). The post-2015 positive trend would have remained negative (−0.25 ppb year^{-1}) if fire impacts were removed, suggesting that fires are the major driver of the national trend reversal. We quantified the mitigation progress offset by wildfires as the ratio of fire-enhanced O_3 during 2015–2024 to the O_3 reduction achieved during 2003–2015, which shows that fires have erased an equivalent of 3.9 years of mitigation progress nationally since 2015. Importantly, fig. S3 shows that this national trend reversal is not captured by analyses based on long-term continuous EPA monitoring stations because of their limited spatial coverage. Analyses based directly on CAMS also differ from observation-informed MLP results, suggesting a much slower national O_3 reduction during 2003–2015 and not capturing the dip during the COVID-19 pandemic in 2020–2021, likely because of the prescribed anthropogenic emission reduction pathway used in the CAMS model (fig. S3).

Regionally, wildfire emissions have reversed policy-relevant O_3 trends since 2015 in the western US and the Midwest (Fig. 2, D and E; regions outlined in Fig. 2A). In the western US, trends reverse from −0.44 ppb year^{-1} during 2003–2015 to +0.13 ppb year^{-1} during 2015–2024 (+0.16 ppb year^{-1} when the COVID-19 period is excluded). If wildfire impacts were excluded, the MLP-derived trend would have remained negative (−0.22 ppb year^{-1}), indicating the dominant role of wildfires in driving the reversal. Wildfire emissions have offset ~6.2 years of mitigation efforts in the western US since 2015. This regional trend reversal is not captured by analyses based on sparse EPA stations, which instead show a continuing negative trend (fig. S3). Indeed, long-term continuous monitoring stations are disproportionately located along coastal regions, whereas inland station coverage is comparatively sparse (Fig. 1A). Because the trend reversal primarily takes place in inland regions such as the Northern Rockies (Fig. 2, A and B), regional averages derived from station data underrepresent these changes. CAMS-based analyses suggest a near-flat trend (+0.03 ppb year^{-1}) in the western US during 2003–2015 and do not reflect the trend reversal since 2015 identified by MLP (fig. S3). In the Midwest, the policy-relevant O_3 trend shifts

from −0.54 ppb year^{-1} during 2003–2015 to +0.26 ppb year^{-1} during 2015–2024 (+0.36 ppb year^{-1} when the COVID-19 period is excluded). Excluding wildfire impacts would result in a continued decrease of −0.30 ppb year^{-1}, suggesting a fire-driven trend reversal. Wildfires have eroded about 5.3 years of mitigation efforts in the Midwest since 2015.

Grid-level analysis further reveals that the trend reversal is geographically widespread (Fig. 2, A and B). During 2003–2015, policy-relevant O_3 declined at statistically significant rates (>1 ppb year^{-1}) across California, the Northern Rockies, the Great Lakes region, and the eastern US, with decreases prevailing over most regions except parts of the central US and the Intermountain West (e.g., Uinta Basin). By contrast, during 2015–2024, trends reversed across much of the western and central US, particularly in the Northern Rockies, where wildfire activity is frequent. Positive trends are also observed over most of the Midwest, reflecting the increasing influence from the long-range transport of wildfire emissions. Notably, grid-level trends from MLP show stronger agreement with EPA station-level trends than those derived directly from CAMS, with higher accuracy in trend direction (98.3 versus 92.0% during 2003–2015 and 88.3 versus 61.2% during 2015–2024; fig. S4).

Finally, we estimated trends of annual premature deaths attributable to long-term fire-sourced O_3 exposure. We estimated premature mortality due to chronic all-sourced O_3 exposure by convolving MLP-predicted warm-season (April to September) average MDA8 with population data and baseline mortality rates (methods). We derived counterfactual mortality using "no-fire" O_3 levels based on the GEOS-Chem modeling approach, and the difference between the two scenarios represents fire-related mortality. As the Global Fire Emissions Database emissions used in our GEOS-Chem simulations have not yet been updated to 2024 as of this writing, the analysis covers 2003–2023.

We found that, nationally, premature deaths attributable to long-term fire-sourced O_3 exposure have increased significantly since 2013 (+318 deaths per year). The annual average mortality during 2013–2023 is 46% higher than that during 2003–2013. The most severe years are 2023 (7974 deaths), 2021 (5737 deaths), and 2020 (3996 deaths). Regionally, the western US has shown a pronounced upward trend since 2013 (+87 deaths per year), with the highest mortality in 2020 (2109 deaths), followed by 2021 (2067 deaths) and 2018 (1797 deaths). Average annual premature deaths during 2013–2023 are 71% higher than during 2003–2013 in the western US. The Midwest also exhibits a statistically significant increase (+89 deaths per year), peaking in 2023 (2417 deaths) and 2021 (1413 deaths). These results underscore the escalating public health burden of wildfire-driven O_3 pollution, highlighting the urgent need for integrated strategies to reduce both anthropogenic and fire emissions to sustain progress in O_3 air quality and mortality reduction.

Challenges in meeting and lowering O_3 standards

We assessed the recent status (2022–2024) of meeting NAAQS and examined the feasibility of adopting a more stringent O_3 standard in the context of increasing wildfire emissions. Under the existing 2015 NAAQS, the health-based standard is 70 ppb. However, epidemiological studies have reported increased mortality and morbidity even below this threshold (*29*). The World Health Organization recommends a more stringent short-term guideline of 50 ppb, with an interim target of 60 ppb (*30*). It is worth noting that our evaluation strategy explicitly considers wildfire-related exceedances, whereas the EPA treats them as exceptional natural events (*31*). However, the growing frequency and severity of wildfires (*2*), largely driven by anthropogenic climate change, may warrant a reevaluation of this exemption policy to better protect public health.

The recent period (2022–2024) includes the long-range transport events of the 2023 Canadian wildfire smoke, providing a critical challenge for complying with NAAQS. We first examined the impact of the 2023 Canadian wildfires on O_3 exceedance days and compared it with the 2020–2022 period (Fig. 3, A and B). During 2020–2022, 21% of the CONUS population (70 million people) lived in areas above the existing 70-ppb standard (annual exceedance days >3, which led to annual fourth-highest MDA8 exceeding 70 ppb). At that time, 64, 8, and 2% of the population were exposed to at least 1 day, 1 week, and 1 month of exceedance, respectively. Southern California experienced the highest exceedance levels (>1 month), with week-long exceedances also observed in the urban areas of Arizona and Colorado, as well as the Permian Basin. Exceedances of more than 3 days were also common in urban Texas, the Lake Michigan region, and New York City. However, the 2023 Canadian wildfire smoke substantially worsened O_3 pollution, with 44% of the population (148 million people) residing in areas above the existing 70-ppb standard (annual exceedance days >3). At that time, 74, 25, and 2% of the population experienced at least 1 day,

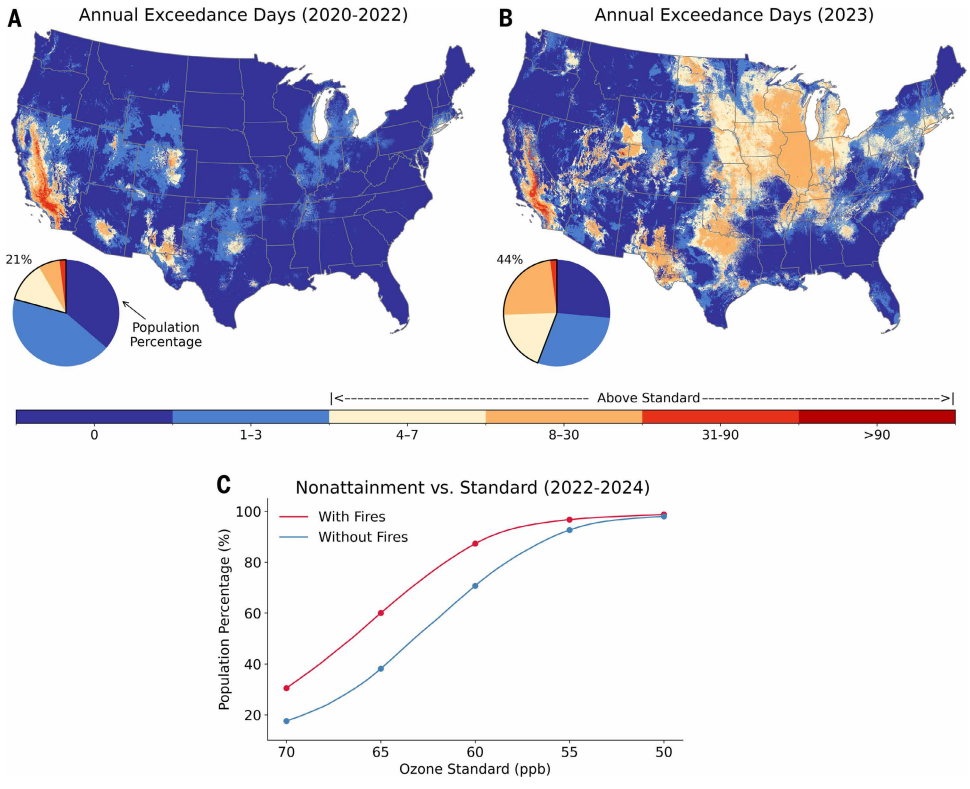

Fig. 3. Challenges in meeting and lowering O_3 standards under growing fire impacts. (**A**) Average annual exceedance days during 2020–2022 under the existing 2015 NAAQS (70 ppb). Inset pie charts show the population distribution by exceedance day, with annotated percentages above standard (annual exceedance days >3). (**B**) Same as (A) but for 2023, the year influenced by the Canadian wildfire. (**C**) Percentage of CONUS population living in nonattainment areas under various O_3 standards during 2022–2024 (defined using 3-year average annual fourth-highest MDA8 levels). Red lines represent MLP-predicted results, and blue lines show counterfactual estimates without fire impacts.

1 week, and 1 month of exceedance, respectively. Widespread exceedances occurred across the Midwest (>1 week), with impacts extending into the Northeast (e.g., New York) and the Deep South (e.g., Texas and Georgia).

We further evaluated the feasibility of lowering O_3 standards during 2022–2024 (Fig. 3C). Under the existing 70-ppb standard, 30% of the population (102 million people) lived in nonattainment areas, a fraction that would decline to 17% if wildfire impacts were removed. The population living in nonattainment was comparable to that under a hypothetical 66-ppb standard if there were no wildfire impacts, indicating that wildfires effectively prevent the US from lowering its O_3 standard by about 4 ppb. In the presence of wildfire impacts, if the O_3 standard were lowered to 65 ppb, 60% of the population (202 million people) would fall into nonattainment, and under a 60-ppb standard, the fraction would increase to 87% (294 million people). These findings demonstrate the challenge in adopting a more stringent O_3 standard as growing wildfires contribute to high O_3 episodes.

Conclusions

Growing wildfire emissions from the western US and Canada have substantially elevated surface O_3 levels across CONUS. However, full-coverage MDA8 O_3 datasets remain lacking for high-fire years after 2016, limiting assessments of fire impacts on regulatory compliance and public health. Here, we addressed this gap by developing a full-coverage daily MDA8 O_3 dataset at 1-km resolution from 2003 to 2024 using deep learning, with demonstrated strong skills in capturing exceedance events of NAAQS. The full-coverage ML-based results reveal a reversal in national O_3 trends after 2015 that is not captured by the sparse EPA monitoring network. Policy-relevant O_3 levels declined by 0.65 ppb $year^{-1}$ during 2003–2015 owing to declining anthropogenic emissions but increased by 0.13 ppb $year^{-1}$ during 2015–2024 as a result of increasing wildfire emissions. Regional fire-driven trend reversals are found in the western US and the Midwest, where 6.2 and 5.3 years of mitigation progress are negated. Premature deaths from chronic exposure to fire-sourced O_3 have increased significantly by 318 deaths per year since 2013, with post-2013 mortality 46% higher than pre-2013 mortality. The most severe years are 2023 (7974 deaths), 2021 (5737 deaths), and 2020 (3996 deaths). During 2022–2024, wildfire emissions led to an additional 43 million people living in nonattainment areas, effectively preventing the US from tightening its O_3 standard by 4 ppb. Escalating challenges in O_3 regulation and public health protection are expected as wildfire emissions continue to increase under climate change (*2*, *32*, *33*). Mitigating climate change and implementing fire prevention measures can lead to improved standards in air quality and potentially bring large benefits to public health.

REFERENCES AND NOTES

1. US Environmental Protection Agency (EPA), Ozone Trends; https://www.epa.gov/air-trends/ozone-trends [accessed October 2025].
2. B. Byrne *et al.*, *Nature* **633**, 835–839 (2024).
3. H. Lee, D. A. Jaffe, *Environ. Sci. Technol.* **58**, 14764–14774 (2024).
4. J. Wei *et al.*, *Lancet Planet. Health* **7**, e963–e975 (2023).
5. O. R. Cooper *et al.*, *Geophys. Res. Lett.* **51**, e2024GL111481 (2024).
6. M. Burke *et al.*, *Nature* **622**, 761–766 (2023).
7. EPA, Review of the Ozone National Ambient Air Quality Standards, 40 C.F.R. pt. 50, *Fed. Reg.* **85**, 87256–87351 (2020); https://www.govinfo.gov/content/pkg/FR-2020-12-31/pdf/2020-28871.pdf.
8. EPA, Green Book 8-Hour Ozone (2015) Area Information (2024); https://www.epa.gov/green-book/green-book-8-hour-ozone-2015-area-information.
9. K. M. Seltzer, D. T. Shindell, C. S. Malley, *Environ. Res. Lett.* **13**, 104018 (2018).
10. S. C. Anenberg, L. W. Horowitz, D. Q. Tong, J. J. West, *Environ. Health Perspect.* **118**, 1189–1195 (2010).
11. K. L. Chang, B. C. McDonald, C. Harkins, O. R. Cooper, *Atmos. Chem. Phys.* **25**, 5101–5132 (2025).
12. S. Dinavahi, C. L. Archer, *Bull. Atmos. Sci. Technol.* **6**, 6 (2025).
13. Q. Di, S. Rowland, P. Koutrakis, J. Schwartz, *J. Air Waste Manag. Assoc.* **67**, 39–52 (2017).
14. W. J. Requia *et al.*, *Environ. Sci. Technol.* **54**, 11037–11047 (2020).
15. L. Xu *et al.*, *Sci. Adv.* **7**, eabl3648 (2021).
16. A. Inness *et al.*, *Atmos. Chem. Phys.* **19**, 3515–3556 (2019).
17. K. Sims *et al.*, *LandScan Global 2022* (Oak Ridge National Laboratory, 2023).
18. C. D. Elvidge, K. Baugh, M. Zhizhin, F. C. Hsu, T. Ghosh, *Int. J. Remote Sens.* **38**, 5860–5879 (2017).
19. K. Didan, MYD13A3 MODIS/Aqua Vegetation Indices Monthly L3 Global 1km SIN Grid V006. EarthData (2015); https://doi.org/10.5067/MODIS/MYD13A3.006.
20. ASTER Team, ASTER Global Digital Elevation Model V003. EarthData (2019); https://doi.org/10.5067/ASTER/ASTGTM.003.
21. M. Friedl, D. Sulla-Menashe, MCD12Q1 MODIS/Terra+Aqua Land Cover Type Yearly L3 Global 500m SIN Grid V006. EarthData (2019); https://doi.org/10.5067/MODIS/MCD12Q1.006.
22. J. Wang *et al.*, *Remote Sens. Environ.* **237**, 111466 (2020).
23. H. Tran *et al.*, *Geohealth* **8**, GH000938 (2024).
24. B. Dix *et al.*, *Geophys. Res. Lett.* **47**, e2019GL085866 (2020).
25. R. Xu *et al.*, *Nature* **621**, 521–529 (2023).
26. Q. Zhang *et al.*, *Nature* **645**, 672–678 (2025).
27. J. He *et al.*, *PNAS Nexus* **3**, pgad483 (2024).
28. L. N. Lamsal *et al.*, *Atmos. Environ.* **110**, 130–143 (2015).
29. Q. Di *et al.*, *N. Engl. J. Med.* **376**, 2513–2522 (2017).
30. World Health Organization (WHO), "World Health Organization global air quality guidelines; Particulate matter ($PM_{2.5}$ and PM_{10}), ozone, nitrogen dioxide, sulfur dioxide and carbon monoxide" (WHO, 2021); https://www.who.int/publications/i/item/9789240034228.
31. O. R. Cooper, A. O. Langford, D. D. Parrish, D. W. Fahey, *Science* **348**, 1096–1097 (2015).
32. A. Clayton, "LA fires forecast to be costliest blaze in US history with estimate of over $200bn in losses," *Guardian*, 13 January 2025; https://www.theguardian.com/us-news/2025/jan/13/la-fires-wildfire-economic-losses.
33. S. Neuman, "Smoke knows no boundaries: What Canada's fires mean for the U.S. in the future," NPR, 6 June 2025; https://www.npr.org/2025/06/06/nx-s1-5424434/wildfires-canada-u-s-climate-change.
34. W. Deng, J. Wang, M. Zhou, L. Rouil, High-resolution (1 km) surface MDA8 ozone dataset over the Continental USA (2003–2024). Zenodo (2025); https://doi.org/10.5281/zenodo.17502917.
35. Ulowa AER Lab, Downscaled CAMS ozone analysis code. Zenodo (2026); https://doi.org/10.5281/zenodo.19039436.

ACKNOWLEDGMENTS

We acknowledge all institutions for the public availability of their data. **Funding:** This work was supported by NASA's Terra, Aqua, and Suomi National Polar-orbiting Partnership (SNPP) program (grant 80NNSC21L1976 to J.Wa.), NASA's Modeling and Analysis program (grant 80NSSC21K1494 to J.Wa.), NASA's Health and Air Quality program (grant 80NSSC22K1047 to J.Wa.), and the NSF's Established Program to Stimulate Competitive Research (EPSCoR) program (award 2420405 to J.Wa.). **Author contributions:** Conceptualization: J.Wa.; Methodology: W.D., M.Z., J.Wa., X.C., X.W., J.We., H.Z.; Investigation: W.D., J.Wa., M.Z.; Visualization: W.D.; Funding acquisition: J.Wa.; Supervision: J.Wa., M.Z.; Writing – original draft: W.D., J.Wa.; Writing – review & editing: M.Z., X.C., X.W., H.Z., J.We., J.B.C., A.d.S., C.G., G.P.B., L.R. **Competing interests:** The authors declare that they have no competing interests. **Data, code, and materials availability:** The long-term high-resolution US surface MDA8 O_3 dataset generated in this study is available at Zenodo (*34*). All datasets used for ML training are publicly available. EPA MDA8 O_3 measurements can be accessed at https://aqs.epa.gov/aqsweb/airdata/download_files.html. CAMS atmospheric composition reanalysis is downloadable at https://ads.atmosphere.copernicus.eu/datasets/cams-global-reanalysis-eac4. VIIRS nighttime light data can be downloaded at https://ladsweb.modaps.eosdis.nasa.gov/missions-and-measurements/products/VNP46A4/. LandScan population count can be downloaded at https://landscan.ornl.gov/. MODIS NDVI can be accessed at https://www.earthdata.nasa.gov/data/catalog/lpcloud-myd13a3-061. CERES shortwave flux can be downloaded at https://ceres.larc.nasa.gov/data/. ERA5 reanalysis is available at https://cds.climate.copernicus.eu/datasets/reanalysis-era5-pressure-levels?tab=download and https://cds.climate.copernicus.eu/datasets/reanalysis-era5-land?tab=download. ASTER elevation can be downloaded at https://asterweb.jpl.nasa.gov/gdem.asp. MODIS land type can be downloaded at https://ladsweb.modaps.eosdis.nasa.gov/missions-and-measurements/products/MCD12Q1. All data analyses and visualizations were conducted using Python, deposited at Zenodo (*35*). No new materials were generated for this study.

SUPPLEMENTARY MATERIALS

science.org/doi/10.1126/science.aed3197
Materials and Methods; Supplementary Text; Figs. S1 to S8; Tables S1 to S3; References (*36*–*65*)

Submitted 23 October 2025; accepted 3 April 2026

10.1126/science.aed3197